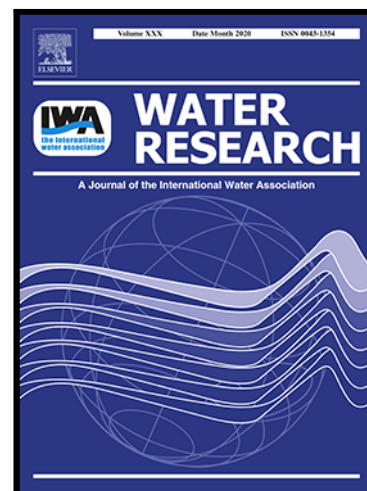


Journal Pre-proof

Microbial Stratification and DOM Removal in Drinking Water Biofilters: Implications for Enhanced Performance

Xiang Shi , Ryan Pereira , Uzma , Laurie Savage ,
Baptiste Poursat , Dominic Quinn , Anastasiia Kostyrsia ,
Fabien Cholet , Cindy J Smith , Caroline Gauchotte-Lindsay ,
William T. Sloan , Umer Ijaz , Marta Vignola

PII: S0043-1354(24)00953-9
DOI: <https://doi.org/10.1016/j.watres.2024.122053>
Reference: WR 122053



To appear in: *Water Research*

Received date: 5 February 2024
Revised date: 9 May 2024
Accepted date: 4 July 2024

Please cite this article as: Xiang Shi , Ryan Pereira , Uzma , Laurie Savage , Baptiste Poursat , Dominic Quinn , Anastasiia Kostyrsia , Fabien Cholet , Cindy J Smith , Caroline Gauchotte-Lindsay , William T. Sloan , Umer Ijaz , Marta Vignola , Microbial Stratification and DOM Removal in Drinking Water Biofilters: Implications for Enhanced Performance, *Water Research* (2024), doi: <https://doi.org/10.1016/j.watres.2024.122053>

This is a PDF file of an article that has undergone enhancements after acceptance, such as the addition of a cover page and metadata, and formatting for readability, but it is not yet the definitive version of record. This version will undergo additional copyediting, typesetting and review before it is published in its final form, but we are providing this version to give early visibility of the article. Please note that, during the production process, errors may be discovered which could affect the content, and all legal disclaimers that apply to the journal pertain.

© 2024 Published by Elsevier Ltd.

Highlights

- Microbial communities at the opposite ends of a biofilter are compositionally different
- The bottom community shows greater network complexity
- Both communities can rapidly degrade labile carbon fractions
- Complex, refractory carbon degradation is exclusive to the bottom community

Journal Pre-proof

Microbial Stratification and DOM Removal in Drinking Water Biofilters: Implications for Enhanced Performance

Xiang Shi ^a, Ryan Pereira ^b, Uzma ^a, Laurie Savage ^a, Baptiste Poursat ^a, Dominic Quinn ^a, Anastasiia Kostrytsia ^a, Fabien Cholet ^a, Cindy J Smith ^a, Caroline Gauchotte-Lindsay ^a, William T. Sloan ^a, Umer Ijaz ^a, Marta Vignola ^{a,*}

^a University of Glasgow, James Watt School of Engineering, Advanced Research Centre (ARC), Chapel Lane, Glasgow G11 6EW (UK)

^b The Lyell Centre, Heriot-Watt University, Research Avenue South, Edinburgh, EH14 4AP (UK)

* Corresponding author: marta.vignola@glasgow.ac.uk

Keywords: Drinking water biofilters; Dissolved organic matter (DOM) removal; Microbial stratification; Granular activated carbon (GAC)

ABBREVIATIONS

DOM: Dissolved Organic Matter

DOC: Dissolved Organic Carbon

DON: Dissolved Organic Nitrogen

BP: Biopolymer

HS: Humic Substances

BB: Building Blocks

LMWN: Low Molecular Weight Neutrals

LMWA: Low Molecular Weight Acid

GAC: Granular Activated Carbon

LC-OCD: Liquid Chromatography-Organic Carbon Detector

TOC: Total Organic Carbon

NTI: Nearest Taxon Index

PBS: Phosphate Buffer Saline

PES: Polyethersulfone

HSD: honestly significant difference

PCoA: Principal Coordinates Analyses

ABSTRACT

Biofiltration is a low-cost, low-energy technology that employs a biologically activated bed of porous medium to reduce the biodegradable fraction of the dissolved organic matter (DOM) pool in source water, resulting in the production of drinking water. Microbial communities at different bed depths within the biofilter play crucial roles in the degradation and removal of dissolved organic carbon (DOC), ultimately impacting its performance. However, the relationships between the composition of microbial communities inhabiting different biofilter depths and their utilisation of various DOC fractions remain poorly understood. To address this knowledge gap, we conducted an experimental study where microbial communities from the upper (i.e., top 10 cm) and lower (i.e., bottom 10 cm) sections of a 30-cm long laboratory-scale biofilter were recovered. These communities were then individually incubated for 10 days using the same source water as the biofilter influent. Our study revealed that the bottom microbial community exhibited lower diversity yet had a co-occurrence network with a higher degree of interconnections among its members compared to the top microbial community. Moreover, we established a direct correlation between the composition and network structure of the microbial communities and their ability to utilise various DOM compounds within a DOM pool. Interestingly, although the bottom microbial community had only 20% of the total cell abundance compared to the top community at the beginning of the incubation, it utilised and hence removed approximately 60% more total DOC from the DOM pool than the top community. While both communities rapidly utilised labile carbon fractions, such as low-molecular-weight neutrals, the utilisation of more refractory carbon fractions, like high-molecular-weight humic substances with an average molecular weight of more than ca. 1451 g/mol, was exclusive to the bottom microbial community. By employing techniques

that capture microbial diversity (i.e., flow cytometry and 16S rRNA amplicon sequencing) and considering the complexities of DOM (i.e., LC-OCD), our study provides novel insights into how microbial community structure could influence the microbial-mediated processes of engineering significance in drinking water production. Finally, our findings could offer the opportunity to improve biofilter performances via engineering interventions that shape the compositions of biofilter microbial communities and enhance their utilisation and removal of DOM, most notably the more classically humified and refractory DOM compound groups.

INTRODUCTION

Dissolved organic matter (DOM) is a complex mixture of organic compounds derived from diverse biological and physical processes (McDowell, 2022). DOM in water is commonly quantified using the elemental content of its collective components, for example, in the form of dissolved organic carbon (DOC) or dissolved organic nitrogen (DON) concentrations (Yates et al., 2019). DOM is ubiquitous at measurable concentrations in both groundwater and surface water, which are the main sources of drinking water. DOM reduces the biostability of drinking water, promotes the growth of microorganisms within water distribution systems, and leads to the formation of undesired disinfection by-products (DBP) during disinfection (Kaarela et al., 2021; Park et al., 2016). Effective reduction of DOM concentration early in the drinking water treatment train is of paramount importance.

Biofilters are widely used to remove DOM from the source water before the final stages of disinfection and distribution. These systems do not uniformly eliminate all DOM compound groups within the DOM pool. While certain compounds, such as sugars, amino acids, and organic acids, prove easily usable by microbial communities, the larger polymeric compounds are typically

more resistant to biological degradation, thus potentially requiring the participation of diverse microbial populations and complex enzymatic hydrolysis for their breakdown (Chróst and Rai, 1993). Studies focusing on both surface water and groundwater microbial communities have established direct relationships between the compositions of a microbial community and its ability to utilise distinct compounds within the DOM pool (Logue et al., 2016; Wu et al., 2018). While the various populations within a given microbial community might exhibit preferences for utilising specific DOM compounds (Chen et al., 2023), from a collective standpoint, microbial communities tend to initially prioritise the utilisation of relatively labile DOM only to turn towards more refractory DOM when the labile reservoirs are depleted (Vignola et al., 2023; Wu et al., 2018). The (bio)transformation of DOM imposes a selective pressure upon microbial communities, prompting adaptive responses that drive the succession of the microbial community towards a composition capable of utilising a wide spectrum of DOM fractions encompassing both labile and refractory constituents (Ortega-Retuerta et al., 2021; Wu et al., 2018). In the context of biofilters, although direct evidence may be limited, prior investigations have postulated a discernible link between the compositions of the biofilter microbial community and its ability to preferentially utilise specific DOM fractions (e.g., specific trihalomethane precursors) and adapt to changing constituents present within the DOM pool (Vignola et al., 2018b).

In recent years, great efforts have been undertaken to study the complex compositions of the biofilter microbial community and its assembly processes throughout the operational lifespan of biofilters (Chen et al., 2021a; Li et al., 2021), as well as to elucidate the influential engineering factors shaping their assembly (Ma et al., 2020; Moona et al., 2021). While the biofilter microbial community compositions and taxa distributions tend to be site- and study-specific, many have shown a ubiquitous ecological pattern characterised by a distinct stratification of the microbial

community within the biofilter along the bed depth that encompasses variations in microbial abundance, diversity, and composition (Boon et al., 2011; Chen et al., 2021b). However, to our knowledge, no explicit investigations have yet discerned a direct association between the stratified compositions of microbial communities at distinct biofilter bed depths and their capability to utilise specific DOM compound groups. A better understanding of the complex and dynamic interplay between the biofilter bed depths, the compositions of microbial communities inhabiting these niches, and their functional traits to selective and preferential use diverse DOM compounds holds the key to designing innovative and more efficient biofilters and improving the current practices for DOM management in safe drinking water production.

To fill this knowledge gap, the research here aims to determine if and how the compositional stratification of the microbial communities over the depth of a biofilter correlates to their functional traits of utilising different DOM fractions within a given DOM pool. We collected GAC material colonised by microbial communities from the upper (top 10 cm) and lower (bottom 10 cm) segments of laboratory-scale GAC biofilters (30 cm) that had been in continuous down-flow operation for a period of 12 weeks. We incubated the recovered GAC material from the two sections in separate batch-mode incubation lasting 10 days. During the incubation, we analysed the two different microbial communities by comparing their composition and co-occurrence networks. This allowed us to identify differences in diversity, composition, and co-occurrence network structure, leading to implications about their respective functionality in utilising different DOM fractions. Additionally, we monitored cell abundance on the GAC surface and changes in the concentrations of various DOM fractions. This provided direct evidence of the two communities' contrasting behaviour in utilising different DOM fractions, validating the functionality implications drawn from our microbial community analysis.

MATERIAL AND METHODS

Laboratory-scale biofilter operation and GAC collection

Three laboratory-scale biofilters packed with GAC (Norit® GAC 1240), each with a length of 30 cm and 2.6 cm internal diameter, were operated in a down-flow mode for 12 weeks at room temperature with an empty bed contact time (EBCT) of 3 hours. The water used for the biofilter operation was sourced from a local freshwater reservoir (Pateshill Water Treatment Works, Scottish Water, United Kingdom). Immediately upon collection, the water was filtered through 10 µm polypropylene cartridge filters (Spectrum, UK) and stored in acid-washed and 18.2 M Ohm deionised water rinsed jerry cans at 4 °C until its use. Upon the completion of the 12 weeks of operation, the biofilters were disassembled, and the GAC from both the upper (0-10 cm) and lower (20-30 cm) segments of each biofilter was recovered separately. The recovered GAC was then transferred to 15 mL centrifuge tubes and centrifuged at 5000 rpm to remove pore water. Thereafter, the GAC from the upper and lower sections of all biofilters were pooled separately into 50 mL centrifuge tubes, yielding two separate batches of GAC, herein referred to as “TOP” and “BOT”, respectively. To ensure the GAC samples remained adequately hydrated throughout the storage process, 5 mL of sterile Phosphate Buffered Saline (PBS; pH=7.2) was added to each 50 mL centrifuge tube containing the pooled GAC. The tubes were gently agitated and inverted by hand to homogenise the GAC. The homogenised GAC samples were stored at 4 °C for approximately 1 month until further use.

Experiment set-up

The experimental design employed a sacrifice batch incubation approach. The treatment groups, referred to as the T groups, were prepared by dispensing 1 g of GAC from TOP or 3.5 g of GAC from BOT into 125 mL serum bottles filled with 60 mL of pre-filtered water as the incubation medium. The water was obtained from the same reservoir used for the biofilter operation, filtered through 10 µm polypropylene cartridge filters on-site, stored at 4 °C in jerry cans, and filtered through 0.2 µm polyethersulfone (PES) membrane filters (Fisher brand, UK) before use. The medium was further amended with ammonium sulphate ((NH₄)₂SO₄) and PBS to reach a C: N: P mass ratio of approximately 100:10:2. This ensures the amount of N, P contents in the medium were higher than the required amount to reach an ideal C: N: P mass ratio of 100: 7: 1 (Qin and Hammes, 2021), thus avoiding limiting the microorganisms with nitrogen or phosphorus. Different weights of GAC were used for TOP and BOT bottles to allow a similar total number of cells between the two groups at the beginning of the experiment. This adjustment ensured that any observed difference in diversity, composition, and DOM removal efficiency between the TOP and BOT batches during the study could not be attributed to disparities in their initial biomass (Cao et al., 2022). The serum bottles were sealed with autoclaved butyl rubber stoppers, and a needle was pierced through the rubber stopper with a 0.2 µm PES membrane filter installed to allow for air exchange between the headspace of the serum bottles and the atmosphere. The serum bottles were wrapped in aluminium foil to block light exposure, thus preventing DOM photochemical degradation. They were then incubated at 20°C for 10 days on an orbital shaker set to 150 rpm. Control groups, referred to as the C1 groups, were set up to account for the effect of DOM adsorption to GAC. C1 groups were set up using the same GAC and water medium in the same amount and configuration as their corresponding T groups, i.e. 1 g and 3.5 g of GAC for TOP and

BOT, respectively, and 60 mL water medium for both. C1 groups were incubated at 4 °C for 10 days on an orbital shaker at 150 rpm. On day 0, three bottles from TOP and BOT of the T groups were sacrificed immediately after setup, respectively. Subsequently, four TOP and BOT bottles from the T groups were sacrificed on days 2, 4, 7, and 10; three TOP and BOT bottles from the C1 groups were sacrificed on days 2 and 10. Finally, to account for the desorption of DOM from the inoculated GAC, additional control groups were set up, referred to as C2 groups. The C2 groups were prepared using the same GAC and in the same amount as their corresponding T groups, following the same procedure and configuration. The medium for the C2 groups was 60 mL of 18.2 M Ohm deionised water instead of filtered and amended raw water. The serum bottles were incubated at 4 °C for 10 days on an orbital shaker at 150 rpm. Two bottles from TOP and BOT of the C2 groups were sacrificed on days 0, 2 and 10, respectively, resulting in biological duplicates at each time point. Figure S1 demonstrates the details of the experiment design.

DNA extraction, 16S rRNA gene amplicon sequencing and sequencing data processing

Approximately 0.5 g of GAC samples were recovered from all the sacrificed serum bottles; GAC samples were gently washed with 2 mL of PBS prior to extraction. Subsequently, 16S rRNA gene amplicon sequencing targeting the variable region 4 (V4) was undertaken by NU-OMICS (Northumbria University, UK) for all DNA extracts, following the MiSeq procedure described elsewhere (Kozich et al., 2013). Refer to supplementary material S1 for the details of the sequencing procedure. Raw sequences were processed using the QIIME2 pipeline (Bolyen et al., 2019) (supplementary material S2). Raw sequences were submitted to the European Nucleotide Archive (ENA), accession number PRJEB71363.

Microbial community diversity analyses and co-occurrence network analyses

We conducted microbial community diversity analyses and co-occurrence network analyses by including only samples from the T groups with more than 5000 reads. We estimated the compositional alpha diversity and phylogenetic alpha diversity within each sample. The compositional alpha diversity was quantified through Pielou's evenness index, Richness index and Shannon index. For phylogenetic alpha diversity, we calculated the nearest-taxon-index (NTI) index. We evaluated the beta diversity between the TOP and BOT microbial communities as well as between each sample combination. Utilising the taxa presence and absence information, we computed the number of shared and unique taxa between the TOP and BOT microbial communities. Moreover, we quantified the dissimilarity between all sample pairs based on the weighted Unifrac distance and visualised the dissimilarity using a Principal Coordinate Analysis (PCoA) ordination plot. Refer to supplementary materials S3 and S8 for the details of the microbial community diversity analyses and the relevant statistical tests, respectively. Moreover, we constructed microbial co-occurrence networks for the TOP and BOT microbial communities at the family level for all samples from the T groups and not the control groups (C1 and C2), comprising 18 samples each. Each dataset was loaded into the MENA tool accessible at <http://ieg2.ou.edu/MENA> for network generation, and the resulting networks were loaded into the Cytoscape software (version 3.10.0) for visualisation (Shannon et al., 2003) (supplementary material S4).

Measuring total DOC concentration, concentrations of various DOC compound groups and cell counts

We measured the total DOC concentration in samples from the T, C1 and C2 groups using a combustion technique (TOC-L, Shimadzu, Japan) (supplementary material S5). We used the liquid chromatography-organic carbon detection-ultraviolet detection-organic nitrogen detection analyser (LC-OCD-UVD-OND, or LC-OCD for short) to identify and quantify different DOC compound groups in T, C1 and C2 samples (supplementary material S6). We monitored the microbial growth dynamics within the T, C1 and C2 groups by tracking the cell abundance from the GAC over time. Cell abundance was determined using a BD Accuri™ C6 Plus flow cytometer equipped with a laser emitting at 488 nm (100 µl/min flowrate; 50 µl sample analysed) following a procedure detailed elsewhere (Vignola et al., 2018a) (supplementary material S7). Information related to relevant statistical tests and glassware preparation procedures are described in supplementary materials S8 and S9, respectively.

Calculating the microbial DOM removal efficiency for DOC and various DOM fractions.

We adopted the parameter of *microbial DOM removal efficiency* to depict the degree of net DOM removal from the medium by microorganisms. Following the similar definition of “removal efficiency” as detailed elsewhere (Boon et al., 2011), we defined *microbial DOM removal efficiency* as the decrease in DOM concentration due to microbial utilisation during a given period, which is further normalised by the average cell counts for this period. For the TOP and BOT microbial communities, we first calculated concentration changes of DOM fractions due to microbial utilisation using the following equation for the early stage of the incubation (between days 0 and 2) and throughout the entire incubation (between days 0 and 10).

$$DOM_{bio}(t_i) = DOM_{C1_{t_i}} - DOM_{T_{t_i}}$$

Where $DOM_{bio}(t_i)$ refers to the average microbial utilisation of the DOM fraction between days 0 and t_i ; t_i refers to the sampling time (i.e., t_2 =day 2 or t_{10} =day 10); $DOM_{C1_{t_i}}$ and $DOM_{T_{t_i}}$ refers to the average DOM fraction concentration measured in the C1 groups and T groups at t_i . The comprehensive set of DOM fractions assessed included BP, HS, BB, LMWA, and LMWN, hereafter referred to as *BP-bio*, *HS-bio*, *BB-bio*, *LMWA-bio* and *LMWN-bio*, and collectively referred to as *DOM-bio*.

Meanwhile, we calculated the average cell counts for the TOP and BOT microbial communities using the following equation:

$$Average\ cell\ counts\ (t_i) = \frac{TCC_0 + TCC_{t_i}}{2}$$

Where *Average cell counts* (t_i) refers to the average total cell counts between days 0 and t_i ; TCC_0 refers to the average total cell counts on day 0 and TCC_{t_i} refers to the average total cell counts at t_i .

Finally, we normalised the *DOM-bio* against the average cell counts to obtain the *microbial DOM removal efficiency* between days 0 and t_i following the equation:

$$microbial\ DOM\ removal\ efficiency\ (t_i) = \frac{DOM_{bio}(t_i)}{Average\ cell\ counts\ (t_i)}$$

The standard deviations of all the derived parameters were obtained through error propagation.

RESULTS

Microbial communities recovered from various biofilter bed depths differed in their compositions and co-occurrence networks.

Our analyses revealed a clear distinction in the compositional structure between the TOP and BOT microbial communities through compositional and phylogenetic alpha diversity and beta diversity analyses. Compared to the BOT microbial community, the TOP microbial community exhibited a higher degree of compositional alpha diversity than the BOT community, indicated by significantly higher values in Pielou's evenness, Richness and Shannon indexes ($p < 0.001$ in all three cases, t -test; **Figure 1A**). In contrast to the compositional alpha diversity, the TOP microbial community displayed a lower phylogenetic alpha diversity compared to the BOT. The mean NTI index among the TOP samples was not significantly different from 0, while it was significantly higher than 0 ($NTI > 0$, $p < 0.001$, t -test) among the BOT samples (**Figure 1B**).

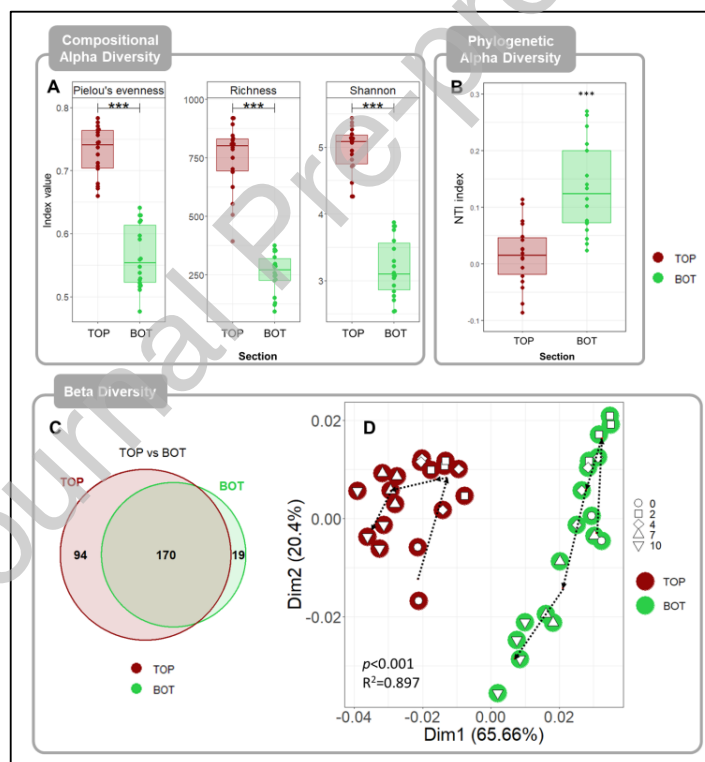


Figure 1. Compositional alpha diversity for TOP and BOT (A), phylogenetic alpha diversity for TOP and BOT (B), Venn diagram based on taxa presence/absence at the family level for TOP and BOT (C), and PCoA plot based on weighted Unifrac distance (D). Only samples belonging to the T groups were analysed. In panel A, the horizontal bars indicate a significant difference in the mean index value between TOP and BOT, and *** indicates $p < 0.001$. In panel B, the *** indicates the mean NTI is significantly different from 0, $p < 0.001$. In panel C, the sizes of the circles are proportional to the number of taxa in TOP and BOT, respectively. In panel D, the dashed lines

connect the centroids of points that belong to the same section (TOP or BOT) and sampling day (days 0, 2, 4, 7 and 10), and the arrowheads indicate the direction of increasing days.

Among all the taxa detected (at the family level), approximately 35% (94/264) of families were uniquely present in the TOP, while only approximately 10% (19/189) of families were uniquely present in the BOT microbial community (**Figure 1C**). This observation suggests that the taxa comprising the BOT community might mostly be seeded from the taxa pool found in the TOP community. Additionally, principal coordinate analysis (PCoA) based on weighted Unifrac demonstrated distinct clusters for the TOP and BOT microbial communities ($p < 0.001$, *PERMANOVA* test; **Figure 1D**), further confirming the compositional differences between the two. TOP and BOT microbial communities also revealed notable differences in their taxa distribution, with the TOP microbial community consistently displayed a lower relative abundance of *Pseudomonadaceae* compared to the BOT for each day (**Figure S2**).

We then assessed the potential interactions within the TOP and BOT communities by constructing their co-occurrence networks and comparing the key network parameters and features. At the family level, a network comprising 109 nodes and 234 links was constructed for the TOP microbial community, and a network consisting of 62 nodes and 462 links was constructed for the BOT microbial community (**Figure 2**). The average degree of the TOP network was only one-third compared to the BOT (4.3 vs. 14.9). The transitivity of the TOP network was considerably lower than the BOT (0.25 vs. 0.49). In both the TOP and BOT networks, most correlations appeared to be positive, with 228 out of 234 connections being positive for the TOP and 456 out of 462 connections being positive for the BOT (**Figure 2**).

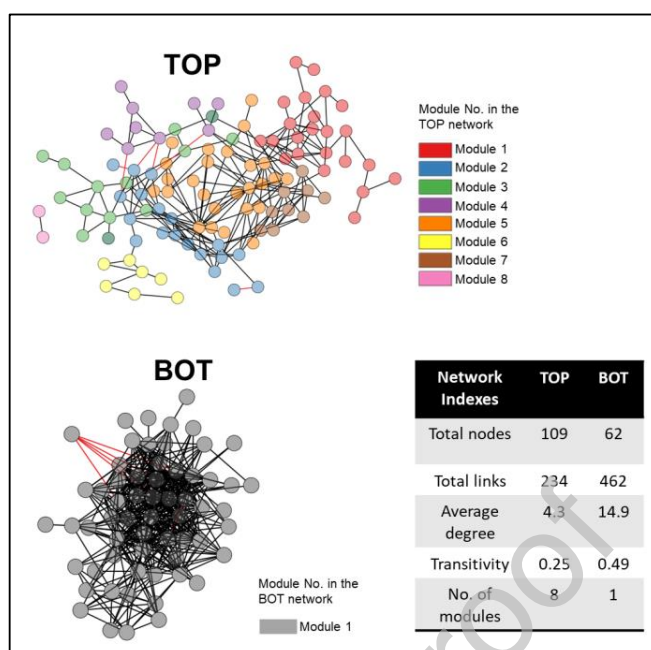


Figure 2. Co-occurrence networks for TOP and BOT microbial communities at the family level. Only samples belonging to the T groups were included in the analysis. Each node represents a taxon at the family level within the network. Node colours indicate the topological module number the underlining taxa were assigned to. Each colour represents one module within the TOP or BOT networks. The line colour indicates the correlation. Black indicates a positive correlation, and red indicates a negative correlation.

BOT microbial community showed higher microbial DOM removal efficiency than the TOP for DOM fractions with larger sizes.

The study of the net DOM removal by the two microbial communities allowed us to obtain direct evidence regarding their utilisation of different DOM fractions.

In the T groups, both TOP and BOT exhibited a decline in DOC concentration during the incubation period (**Figure 3A**). This reduction can be attributed solely to adsorption and microbial degradation, as the effects of photochemical and thermal degradation were minimised by the incubation conditions—specifically, maintaining the samples in the dark and at a constant temperature of 20°C. Specifically, DOC concentrations decreased from ca. 22 ppm on day 0 to ca. 14 ppm on day 10 in the TOP and from ca. 20.5 ppm on day 0 to ca. 8 ppm on day 10 in the BOT

(**Figure 3A**). Meanwhile, cell abundance increased progressively over time, with the TOP showing a rise from ca. 5.7×10^8 cells/g on day 0 to ca. 8.5×10^8 cells/g on day 10 and the BOT showing a rise from ca. 1.4×10^8 cells/g on day 0 to ca. 2.9×10^8 cells/g on day 10 (**Figure 3B**). Statistical analyses confirmed the increase in average cell abundance was statistically significant between days 0 and 4 ($p_{adj} < 0.05$, *Tukey's HSD* test) and between days 0 and 10 ($p_{adj} < 0.001$, *Tukey's HSD* test) for the TOP; and between days 0 and 2 ($p_{adj} < 0.001$, *Tukey's HSD* test) and between days 0 and 10 ($p_{adj} < 0.001$, *Tukey's HSD* test) for the BOT. Therefore, both TOP and BOT microbial communities were actively growing, and hence, the decline in DOC concentration could be at least partially attributed to microbial utilisation. In comparison, the C1 groups also experienced a decrease in DOC concentration over the 10-day incubation, albeit to a lesser degree when compared to their corresponding T group samples (**Figure 3A**). However, the average cell abundance in the C1 groups showed no significant difference between days 0 and 10 for both the TOP and BOT (**Figure 3B**), suggesting the decrease in DOC concentrations for the C1 groups was probably adsorption mediated.

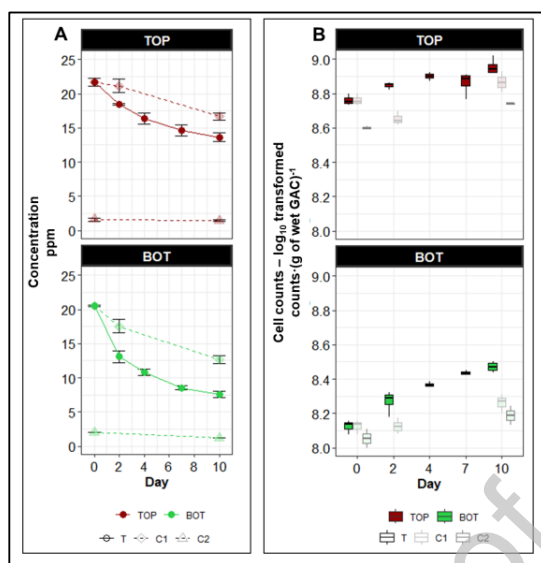


Figure 3. DOC concentration over time (A) and cell count over time (B). In panel A, error bars indicate the standard deviation of the measurements from the biological replicates ($n=4$ for all time points except for day 0 of the T group, $n=3$ for day 0 of the T group and all time points of the C1 group, $n=2$ for all time points of the C2 group).

Next, we examined the concentration change of the five DOM fractions, as characterised by LC-OCD. In the T groups, the concentrations of BP exhibited minimal variation, remaining at ca. 2 ppm for both TOP and BOT throughout the experiment, which was similar to their corresponding C1 groups. This indicates a minimal net removal of BP from the medium. In contrast, concentrations of HS, BB, and LMWN in the T groups demonstrated a consistent decrease over time for both TOP and BOT. Each of these DOM fractions exhibited a distinctive temporal pattern of change in concentrations, both in relation to one another and when compared to their respective C1 groups (**Figure 4A**). Thus, these DOM fractions were removed from the medium at different rates in both TOP and BOT, and the removal could be attributed to microbial utilisation. Furthermore, we evaluated the *microbial DOM removal efficiency* during the early stage of the incubation (between days 0 and 2) and throughout the entire incubation (between days 0 and 10), only accounting for microorganism-mediated net DOM removal (see materials and methods). As the adsorption of bulk DOM is suggested to be exothermic in nature being favoured

at lower temperatures (Moona et al., 2019; Rashed, 2013), we consider the calculated *microbial DOM removal efficiency* a conservative estimation of microbial DOM net utilisation. Furthermore, the results from the BOT section should be considered even more conservative than those from the TOP due to a significantly larger amount of GAC used -3.5 grams compared to 1 gram in the TOP — which likely enhanced the effect of DOM adsorption. During the early stage of the incubation, the *microbial BB removal efficiency* by the BOT community was 5 times greater than the TOP (1.2×10^{-9} ppm·cell⁻¹ vs. 2.4×10^{-10} ppm·cell⁻¹; **Figure 4B**). Similarly, the *microbial HS removal efficiency* by the BOT microbial community was ca. 6.9×10^{-9} ppm·cell⁻¹, approximately 7 times greater than that of the TOP, calculated at ca. 1.0×10^{-9} ppm·cell⁻¹ (**Figure 4B**). Over the entire incubation period, *microbial BB* and *HS removal efficiency* by the BOT community was caught up by the TOP community. Throughout the incubation, the *microbial BB removal efficiency* by the BOT microbial community became 6.1×10^{-10} ppm·cell⁻¹, only 70% of the TOP *microbial BB removal efficiency* (8.7×10^{-10} ppm·cell⁻¹; **Figure 4B**), whereas the *microbial HS removal efficiency* by the BOT microbial community became only 50% greater than the TOP (7.5×10^{-9} ppm·cell⁻¹ vs. 5.0×10^{-9} ppm·cell⁻¹; **Figure 4B**).

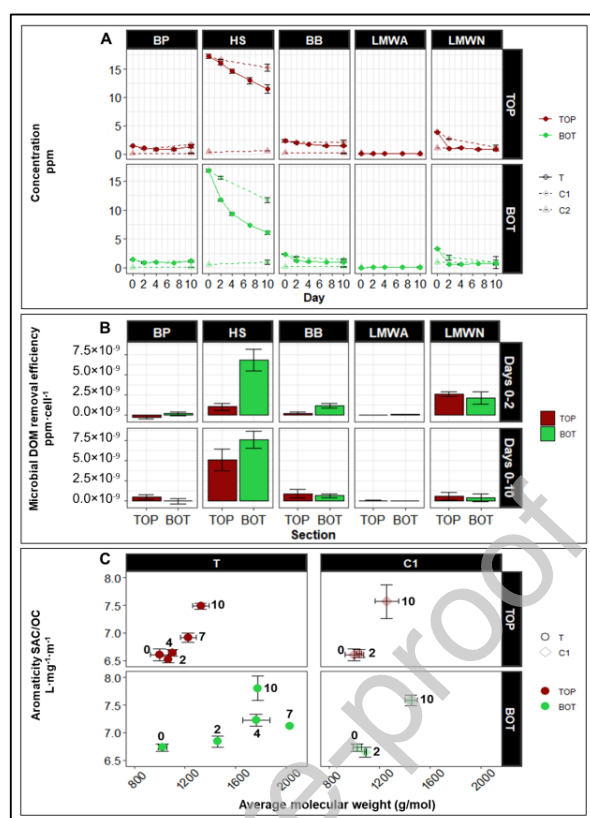


Figure 4. Concentrations of the DOM fractions over time (A), the microbial DOM removal efficiency for the five DOM fractions (i.e. BP, HS, BB, LMWA and LMWN) during the early stage of the incubation (between days 0 and 2), and throughout the entire incubation period (between days 0 and 10) (B), and the HS diagram showing the average molecular weight and aromaticity of the HS fraction within the DOM pool (C). In panels, A and C, the error bars indicate the standard deviation of measurements from the biological replicates ($n=4$ for all time points except for day 0 of the T group, $n=3$ for day 0 of the T group and all time points of the C1 group, $n=2$ for all time points of the C2 group). In panel B, error bars indicate the derived standard deviation following error propagation. In panel C, aromaticity was calculated as the ratio between the spectral absorption coefficient (SAC) and the organic carbon of the humic fraction (OC). The numbers next to the points indicate the days from which the corresponding samples were collected.

We further examined the changes in the average molecular weight and aromaticity within the HS fraction. In the T groups, we observed a shift towards higher average molecular weight over time, and this shift was more pronounced in BOT compared to TOP (**Figure 4C**). For the TOP, the average molecular weight increased from ca. 1001 g/mol on day 0 to ca. 1326 g/mol on day 10, while for the BOT, it increased from ca. 1024 g/mol on day 0 to 1777 g/mol on day 10 (**Figure 4C**). However, a single-time data point on day 7 for the BOT was considered an outlier

due to a temporary instrument issue, so it should be interpreted with caution. In the C1 groups, the average molecular weight for the TOP reached ca. 1260 g/mol on day 10, approximately 60 g/mol lower than its corresponding T groups (ca. 1326 g/mol), whereas the average molecular weight for the BOT reached ca. 1451 g/mol which was approximately 320 g/mol lower than its corresponding T groups (ca. 1777 g/mol; **Figure 4C**). Therefore, our results further indicate that microbial utilisation resulted in a more notable shift in the average molecular weight of HS in BOT compared to TOP.

DISCUSSION

In this work, we observed clear differences in the abundance, community richness, evenness and compositions between the TOP and BOT microbial communities throughout the incubation period (**Figure 1; Figure 3B**). The PCoA analysis indicated that the difference in biofilter depth explained the compositional distinction between the TOP and BOT microbial communities. Conversely, incubation time did not emerge as a statistically significant factor in explaining compositional variations within both TOP and BOT microbial communities (**Figure 1D**). This suggests that the observed difference in the compositional structure between the TOP and BOT microbial communities was mainly introduced by their respective inoculum collected at different depths of the biofilters rather than gradually developed over the 10-day incubation. This further indicates the existence of stratification within the biofilters in the compositional structure of the microbial community, aligning with the abundant observations from other studies (Boon et al., 2011; Chen et al., 2021a; Vignola et al., 2018b).

We observed distinct structures of microbial co-occurrence networks between the TOP and BOT microbial communities. The structure of microbial co-occurrence networks has been linked to the degree of interactions among the community members and their ability to utilise complex

substrates (Chen et al., 2022; Deng and Wang, 2016; Hertkorn et al., 2002; Ostrem Loss et al., 2023). The ability to utilise large and complex substrates, which often require many different enzymes that involve various species (Hertkorn et al., 2002), could be associated with a microbial co-occurrence network that is characterised by a high degree of interconnections among the constituent taxa within the network (Chen et al., 2022) and a large proportion of positive inter-species correlations (Chen et al., 2022; Deng and Wang, 2016; Ostrem Loss et al., 2023). These positive interactions facilitate synergistic growth and limit competition among community members (Deng and Wang, 2016; Ostrem Loss et al., 2023). In our study, both the TOP and BOT microbial networks were dominated by positive correlations between the taxa (**Figure 2**), implying the functional traits to utilise large and complex DOM fractions by both microbial communities. Moreover, the BOT microbial community exhibited a higher degree of inter-species connections within its co-occurrence network than the TOP, as supported by a higher average degree and transitivity. This suggests that the BOT microbial community might be more capable of removing the recalcitrant DOM fractions compared to the TOP.

The implications for the functionality of DOM utilisation by both TOP and BOT microbial communities, which we inferred from the microbial community analysis, aligned with our observations of net DOM removal behaviour. Both TOP and BOT communities demonstrated the ability to microbiologically remove the various DOM fractions (**Figure 4A, B**). The removal of LMWN and BB was consistent with expectations, as these DOM fractions are generally considered labile and easily utilised by microorganisms (Boon et al., 2011). The BOT microbial community exhibited higher microbial BB removal efficiency at the early incubation stage (1.2×10^{-9} ppm·cell⁻¹) than the entire incubation (6.1×10^{-10} ppm·cell⁻¹, **Figure 4B**), possibly due to a depletion of bioavailable BB toward the incubation's end. Conversely, the TOP microbial community showed

lower BB removal efficiency at the early stage (2.4×10^{-10} ppm·cell⁻¹) compared to the entire incubation (8.7×10^{-10} ppm·cell⁻¹, **Figure 4B**), indicating a need for time to increase its active level in BB removal. Interestingly, we did not observe strong evidence of BP utilisation, although BP is generally considered labile (Chen et al., 2016). This lack of BP utilisation was also reported in other similar studies, and the authors attributed it to the formation of BP by the microorganisms during growth. Thus, we speculated that the same reason might apply, and the BP utilisation might be offset by its production, rendering it overall undetected (Vignola et al., 2023).

In our study, HS constituted a substantial proportion of ca. 83% of the total DOC pool, which is consistent with previous reports that HS can make up 50% to 85% of the DOC pool in natural water (Hertkorn et al., 2002). HS are known for their complex and heterogeneous nature, varying widely in sizes and chemical structures. Removing HS has been a major focus in drinking water production, as they have the potential to produce carcinogenic substances following chlorine disinfection (Hertkorn et al., 2002). Despite HS being more recalcitrant in nature, some degree of HS removal was observed by both the TOP and BOT microbial communities (**Figure 4B**). Within the HS pool, the increase in average molecular weight suggests the removal of HS with lower molecular weight from water. Although the precise compositions of HS are still not fully understood, it is known to consist of small and structurally simple components that can be readily utilised by microorganisms such as proteins, polysaccharides, and amino acids, as well as larger and more complex cores that are considered biologically refractory (Finkbeiner et al., 2020). Additionally, abiotic adsorption of organic macromolecules by GAC is known to decrease with increasing molecular sizes (Karanfil et al., 1996). In our study, both microbial utilisation and adsorption clearly contributed to HS removal by the BOT community, resulting in a higher final average molecular weight in the T groups compared to the C1 groups. The results also indicated

that only the BOT microbial community rather than the TOP utilised the HS components with an average molecular weight between ca. 1451 g/mol and ca. 1777 g/mol (**Figure 4C**), thus demonstrating its ability to utilise DOM with a wider molecular weight range than the TOP. Furthermore, we observed a shift towards higher aromaticity over time, with a similar temporal pattern shared between the TOP and BOT samples from both the T and C1 groups, all starting from ca. 6.8 L/(mg*m) to ca. 8 L/(mg*m) on day 10 (**Figure 4C**). This finding suggests that the aliphatic or head groups within the HS molecules were probably removed from the water preferentially, leaving HS cores consisting of aromatic rings. Our observations align with other studies that indicate microbial decomposition of HS more easily occurs for the aliphatic fractions of HS (Yanagi et al., 2002) and abiotic removal is also more significant for aliphatic compounds than aromatics ones, likely due to the steric conformation of the aromatic compounds, which makes affinity to GAC more challenging (Solisio et al., 2001).

Our results suggested a difference in the *microbial DOM removal efficiency* between the TOP and BOT microbial communities, which is related to the sizes or molecular weights of the DOM fractions. DOM fractions with smaller sizes, such as LMWN, were readily utilised by both the TOP and BOT microbial communities (**Figure 4A**). Meanwhile, at the early stage of the incubation, the BOT microbial communities demonstrated higher *microbial removal efficiency* for DOM fractions with larger sizes than the TOP, such as BB and HS, particularly the HS components with higher average molecular weight (**Figure 4B, C**). The higher *microbial DOM removal efficiency* by the BOT community aligned with previous research, where the authors investigated DOC removal efficiency normalised against ATP concentrations at different bed depths of operational biofilters and observed an increase in removal efficiency with increasing bed depths. For instance, at 45 cm of the biofilter, the removal efficiency was approximately three times higher

compared to that at 10 cm (Boon et al., 2011). Moreover, the impact of organic compound sizes on DOM bioavailability has long been recognised. Small and simple organic compounds can be easily transported across the cell membranes and rapidly utilised (MS Weiss et al., 1991), and their utilisation is considered unspecific and widespread among microbial populations. Large and complex organic compounds likely require multiple extracellular cleavages of the individual or interacting ectoenzymes (Schulten, 1996) and the expression of transmembrane transport systems to enable their uptake (Teeling et al., 2012). The functional traits to utilise large and complex organic compounds are more phylogenetically restricted (Renaud and Martiny, 2013). Our results suggest that functional traits necessary to efficiently utilise large and complex organic compounds might be more prevalent and active in the BOT microbial community at the beginning of the batch incubation. This aligns with findings from our previous study, where we incubated cell suspensions derived from GAC recovered from different sections of 90-cm down-flow biofilters. In that study, the utilisation of complex HS after 23 hours of incubation was restricted to the bottom microbial community (Vignola et al., 2023). In our current study, we directly associated the microbial removal of DOM fractions with the original GAC microbial communities from different biofilter depths, thereby minimising potential biases introduced by derived microbial communities. It is noteworthy that the TOP microbial community also utilised and removed BB and HS during the early stage of the incubation, albeit with considerably lower *microbial DOM removal efficiencies* compared to the BOT community. This might suggest that the TOP microbial community was less equipped with active functional traits for utilising complex DOM fractions than the BOT. Furthermore, as our study measured microbial abundance without distinguishing between active and inactive cells, it is also possible that a fraction of the TOP microbial community might have

been inactive, thus also contributing to its lower *microbial DOM removal efficiencies* calculated during the incubation.

Finally, the observed divergence in compositions and co-occurrence network characteristics between the TOP and BOT microbial communities suggests distinct responses to environmental stressors and disparate environmental processes during their respective assemblies within the biofilters. Although quantification of substrate concentrations across the biofilter depths, from which the TOP and BOT communities originated, was not feasible in our work, based on our microbial community analyses and findings in related studies, it is plausible to speculate that differential availability of simple and labile organic compounds at varying biofilter depths served as at least one of the driving factors for the distinct assemblages of these microbial communities. In natural freshwater systems and engineered water systems such as biofilters, depth has been linked to chemical gradients, which drive changes in community compositions (Lin et al., 2012; Wang et al., 2014). DOM turnover in a biofilter expectedly leads to changing availability of various DOM fractions at different bed depths, creating distinct ecological niches (Boon et al., 2011). As water passes through the biofilter, we presume that the TOP microbial community has access to a wide range of bioavailable organic compounds in the DOM pool. The stochastic processes, mainly the dispersal of microorganisms introduced by the influent water, presumably surpass the deterministic process in influencing the microbial assemblage. Consequently, when compared to the BOT microbial community, the TOP microbial community displays a community NTI index that is not significantly different from 0 and exhibits a microbial co-occurrence network with more taxa and fewer interspecies interactions among the taxa, as what was observed in this work (**Figure 1B; Figure 2**). Since microbial communities prefer labile organic compounds to the refractory ones if they have access to both (Wu et al., 2018), we postulate that the TOP microbial community

utilises the simple and labile DOM fractions in water, leaving only the larger and refractory fractions to the downstream, creating a different niche for the BOT microbial community that is limited by the available simple and labile organic compounds. In aquatic ecosystems with a scarcity of simple DOM fractions, microbial communities adapt, and functional traits for the utilisation of large and complex DOM fractions are promoted and maintained (Chen et al., 2022; Ortega-Retuerta et al., 2021). Hence, we hypothesise that the BOT microbial community in the biofilters undergoes succession that is driven by the deterministic force posed by the environmental stress of available organic compounds scarcity. Therefore, the BOT microbial community displays a community NTI index that is significantly different from 0 (**Figure 1B**), exhibits a microbial co-occurrence network with fewer taxa and more interspecies interactions among the taxa (**Figure 2**), and demonstrates functional traits that facilitate the utilisation of refractory organic compounds that the TOP microbial community might not readily express. Subsequently, when provided with a fresh DOM pool containing both labile and refractory DOM fractions, only the BOT microbial community is able to readily utilise the refractory DOM fractions with a wider size range, as indicated by our observations in this work (**Figure 4**).

CONCLUSION

By adopting a novel approach of combining microbial community analyses, co-occurrence network analysis with detailed analyses of various DOM fractions, which provide direct evidence about the DOM utilisation functionality of the microbial community, we demonstrated that microbial communities retrieved from the TOP and BOT of a biofilter exhibited differences in composition and co-occurrence network structure, and these differences may translate into their distinct preference to utilise various DOM fractions and remove those fractions from the DOM

pool. Our microbial community analyses unveiled the stratification in the biofilter microbial community's compositional structure and the unique interspecies interactions within each community. In comparison to the TOP, the BOT microbial community displayed lower diversity but higher interactivity among its members, suggesting its functional traits in utilising the refractory fractions of a DOM pool with a better DOM removal efficiency. These implications aligned with our analyses of the microbial removal of various DOM fractions, which indicated that the BOT microbial community exhibited greater microbial removal efficiency for a broader range of organic compounds than the TOP. This was particularly evident for refractory DOM fractions like HS, both during the early stage (between days 0 and 2) and throughout the 10-day incubation.

In this study, both the TOP and BOT microbial communities originated from the initial seed community introduced by the influent water. Still, they showed contrasting functional traits of DOM utilisation during incubation. Our explanation for these differences is grounded in the adaptation of the biofilter microbial community to specific environmental niches at different biofilter depths, driven by the expected changing availability of DOM fractions. Our findings align with the perspective that DOM utilisation functionality is an ongoing interplay between DOM composition and the metabolic capacity of the microbial community. For future research, validating our proposed assembling process of the TOP and BOT microbial communities in the biofilters by describing the concentrations of different DOM fractions over the biofilter bed depths and identifying the molecular mechanisms responsible for the differential utilisation of refractory DOM by the two communities could be promising avenues. Finally, in drinking water supply management, strategies to enhance trace organic chemical removal during aquifer recharge by manipulating the availability of biodegradable organic carbons and stimulating the soil microbial community have been successfully validated, both in lab-scale and full-scale implementations

(Alidina et al., 2014; Regnery et al., 2016). In light of our findings, we propose similar approaches to optimise biofilter performance. This involves pre-culturing the inlet biofilter microbial community to equip it with the functionality to readily utilise refractory DOM fractions. Exploring the feasibility and potential benefits of implementing such strategies could be a compelling direction for future investigations, contributing to the development of more efficient biofilters with enhanced DOM removal capabilities.

DATA AVAILABILITY

The raw data obtained from the TOC analyser and flow cytometry is accessible through the following link: <http://dx.doi.org/10.5525/gla.researchdata.1562>. Additional raw data can be provided upon request.

ACKNOWLEDGMENTS

We thank J. Bischoff for technical support.

FUNDING SOURCES

This work was supported by the Royal Academy of Engineering under the Research Fellowship Scheme RF/201819/18/198; the EPSRC EP/V030515/1; the Royal Academy of Engineering, Scottish Water Research Chair RCSR171864 and the environmental Biotechnology Network POC202106. R.P. acknowledges financial support to the European Research Council BOOGIE project under the European Union's Horizon 2020 research and innovation programme, grant number 949495.

REFERENCES

Alidina, M., Li, D., Drewes, J.E., 2014. Investigating the role for adaptation of the microbial community to transform trace organic chemicals during managed aquifer recharge. *Water Res* 56, 172–180. <https://doi.org/https://doi.org/10.1016/j.watres.2014.02.046>

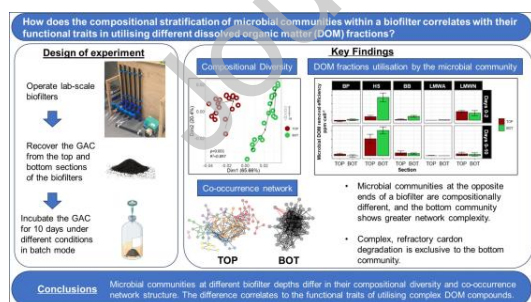
- Bolyen, E., Rideout, J.R., Dillon, M.R., Bokulich, N.A., Abnet, C.C., Al-Ghalith, G.A., Alexander, H., Alm, E.J., Arumugam, M., Asnicar, F., Bai, Y., Bisanz, J.E., Bittinger, K., Brejnrod, A., Brislawn, C.J., Brown, C.T., Callahan, B.J., Caraballo-Rodríguez, A.M., Chase, J., Cope, E.K., Da Silva, R., Diener, C., Dorrestein, P.C., Douglas, G.M., Durall, D.M., Duvallet, C., Edwardson, C.F., Ernst, M., Estaki, M., Fouquier, J., Gauglitz, J.M., Gibbons, S.M., Gibson, D.L., Gonzalez, A., Gorlick, K., Guo, J., Hillmann, B., Holmes, S., Holste, H., Huttenhower, C., Huttley, G.A., Janssen, S., Jarmusch, A.K., Jiang, L., Kaehler, B.D., Kang, K. Bin, Keefe, C.R., Keim, P., Kelley, S.T., Knights, D., Koester, I., Kosciulek, T., Kreps, J., Langille, M.G.I., Lee, J., Ley, R., Liu, Y.-X., Loftfield, E., Lozupone, C., Maher, M., Marotz, C., Martin, B.D., McDonald, D., McIver, L.J., Melnik, A. V, Metcalf, J.L., Morgan, S.C., Morton, J.T., Naimey, A.T., Navas-Molina, J.A., Nothias, L.F., Orchanian, S.B., Pearson, T., Peoples, S.L., Petras, D., Preuss, M.L., Priesse, E., Rasmussen, L.B., Rivers, A., Robeson, M.S., Rosenthal, P., Segata, N., Shaffer, M., Shiffer, A., Sinha, R., Song, S.J., Spear, J.R., Swafford, A.D., Thompson, L.R., Torres, P.J., Trinh, P., Tripathi, A., Turnbaugh, P.J., Ul-Hasan, S., van der Hooft, J.J.J., Vargas, F., Vázquez-Baeza, Y., Vogtman, E., von Hippel, M., Walters, W., Wan, Y., Wang, M., Warren, J., Weber, K.C., Williamson, C.H.D., Willis, A.D., Xu, Z.Z., Zaneveld, J.R., Zhang, Y., Zhu, Q., Knight, R., Caporaso, J.G., 2019. Reproducible, interactive, scalable and extensible microbiome data science using QIIME 2. *Nat Biotechnol* 37, 852–857. <https://doi.org/10.1038/s41587-019-0209-9>
- Boon, N., Pycke, B.F.G., Marzorati, M., Hammes, F., 2011. Nutrient gradients in a granular activated carbon biofilter drives bacterial community organization and dynamics. *Water Res* 45, 6355–6361. <https://doi.org/10.1016/j.watres.2011.09.016>
- Cao, L., Wolff, D., Liguori, R., Wurzbacher, C., Wick, A., 2022. Microbial Biomass, Composition, and Functions Are Responsible for the Differential Removal of Trace Organic Chemicals in Biofiltration Systems: A Batch Study. *Front. Water* 4. <https://doi.org/10.3389/frwa.2022.832297>
- Chen, F., Peldszus, S., Elhadidy, A.M., Legge, R.L., Van Dyke, M.I., Huck, P.M., 2016. Kinetics of natural organic matter (NOM) removal during drinking water biofiltration using different NOM characterization approaches. *Water Res* 104, 361–370. <https://doi.org/10.1016/j.watres.2016.08.028>
- Chen, L., Zhai, Y., van der Mark, E., Liu, G., van der Meer, W., Medema, G., 2021a. Microbial community assembly and metabolic function in top layers of slow sand filters for drinking water production. *J Clean Prod* 294. <https://doi.org/10.1016/j.jclepro.2021.126342>
- Chen, L., Zhai, Y., van der Mark, E., Liu, G., van der Meer, W., Medema, G., 2021b. Microbial community assembly and metabolic function in top layers of slow sand filters for drinking water production. *J Clean Prod* 294. <https://doi.org/10.1016/j.jclepro.2021.126342>
- Chen, M., Hur, J., Gu, J.D., Yamashita, Y., 2023. Microbial degradation of various types of dissolved organic matter in aquatic ecosystems and its influencing factors. *Sci China Earth Sci*. <https://doi.org/10.1007/s11430-021-9996-1>
- Chen, Q., Lønborg, C., Chen, F., Gonsior, M., Li, Y., Cai, R., He, C., Chen, J., Wang, Y., Shi, Q., Jiao, N., Zheng, Q., 2022. Increased microbial and substrate complexity result in higher molecular diversity of the dissolved organic matter pool. *Limnol Oceanogr* 67, 2360–2373. <https://doi.org/10.1002/lno.12206>
- Chróst, R.J., Rai, H., 1993. Ectoenzyme Activity and Bacterial Secondary Production in Nutrient-Im impoverished and Nutrient-Enriched Freshwater Mesocosms. *Microb Ecol* 25, 131–150.

- Deng, Y.J., Wang, S.Y., 2016. Synergistic growth in bacteria depends on substrate complexity. *Journal of Microbiology* 54, 23–30. <https://doi.org/10.1007/s12275-016-5461-9>
- Finkbeiner, P., Moore, G., Pereira, R., Jefferson, B., Jarvis, P., 2020. The combined influence of hydrophobicity, charge and molecular weight on natural organic matter removal by ion exchange and coagulation. *Chemosphere* 238, 124633. <https://doi.org/https://doi.org/10.1016/j.chemosphere.2019.124633>
- Hertkorn, N., Claus, H., Schmitt-Kopplin, P., Perdue, E.M., Filip, Z., 2002. Utilization and transformation of aquatic humic substances by autochthonous microorganisms. *Environ Sci Technol* 36, 4334–4345. <https://doi.org/10.1021/es010336o>
- Kaarela, O., Koppanen, M., Kesti, T., Kettunen, R., Palmroth, M., Rintala, J., 2021. Natural organic matter removal in a full-scale drinking water treatment plant using ClO₂ oxidation: Performance of two virgin granular activated carbons. *Journal of Water Process Engineering* 41. <https://doi.org/10.1016/j.jwpe.2021.102001>
- Karanfil, T., Kilduff, J.E., Schlautman, M.A., Weber, W.J., 1996. Adsorption of Organic Macromolecules by Granular Activated Carbon. 1. Influence of Molecular Properties Under Anoxic Solution Conditions. *Environ Sci Technol* 30, 2187–2194. <https://doi.org/10.1021/es9505863>
- Kozich, J.J., Westcott, S.L., Baxter, N.T., Highlander, S.K., Schloss, P.D., 2013. Development of a dual-index sequencing strategy and curation pipeline for analyzing amplicon sequence data on the miseq illumina sequencing platform. *Appl Environ Microbiol* 79, 5112–5120. <https://doi.org/10.1128/AEM.01043-13>
- Li, L., Ning, D., Jeon, Y., Ryu, H., Santo Domingo, J.W., Kang, D.W., Kadudula, A., Seo, Y., 2021. Ecological insights into assembly processes and network structures of bacterial biofilms in full-scale biologically active carbon filters under ozone implementation. *Science of the Total Environment* 751. <https://doi.org/10.1016/j.scitotenv.2020.141409>
- Lin, X., McKinley, J., Resch, C.T., Kaluzny, R., Lauber, C.L., Fredrickson, J., Knight, R., Konopka, A., 2012. Spatial and temporal dynamics of the microbial community in the Hanford unconfined aquifer. *ISME Journal* 6, 1665–1676. <https://doi.org/10.1038/ismej.2012.26>
- Logue, J.B., Stedmon, C.A., Kellerman, A.M., Nielsen, N.J., Andersson, A.F., Laudon, H., Lindström, E.S., Kritzberg, E.S., 2016. Experimental insights into the importance of aquatic bacterial community composition to the degradation of dissolved organic matter. *ISME Journal* 10, 533–545. <https://doi.org/10.1038/ismej.2015.131>
- Ma, B., Lapara, T.M., Hozalski, R.M., 2020. Microbiome of Drinking Water Biofilters is Influenced by Environmental Factors and Engineering Decisions but has Little Influence on the Microbiome of the Filtrate. *Environ Sci Technol* 54, 11526–11535. <https://doi.org/10.1021/acs.est.0c01730>
- McDowell, W.H., 2022. DOM in the long arc of environmental science: looking back and thinking ahead. *Biogeochemistry*. <https://doi.org/10.1007/s10533-022-00924-w>
- Moona, N., Holmes, A., Wunsch, U.J., Pettersson, T.J.R., Murphy, K.R., 2021. Full-Scale Manipulation of the Empty Bed Contact Time to Optimize Dissolved Organic Matter Removal by Drinking Water Biofilters. *ACS ES and T Water* 1, 1117–1126. <https://doi.org/10.1021/acsestwater.0c00105>

- Moona, N., Wunsch, U.J., Bondelind, M., Bergstedt, O., Sapmaz, T., Pettersson, T.J.R., Murphy, K.R., 2019. Temperature-dependent mechanisms of DOM removal by biological activated carbon filters. *Environ Sci (Camb)* 5, 2232–2241. <https://doi.org/10.1039/c9ew00620f>
- MS Weiss, U Abele, J Weckesser, W Welte, E Schiltz, GE Schulz, 1991. Molecular architecture and electrostatic properties of a bacterial porin. *Science* (1979) 254, 1627–1630.
- Ortega-Retuerta, E., Devresse, Q., Caparros, J., Marie, B., Crispi, O., Catala, P., Joux, F., Obernosterer, I., 2021. Dissolved organic matter released by two marine heterotrophic bacterial strains and its bioavailability for natural prokaryotic communities. *Environ Microbiol* 23, 1363–1378. <https://doi.org/10.1111/1462-2920.15306>
- Ostrem Loss, E., Thompson, J., Cheung, P.L.K., Qian, Y., Venturelli, O.S., 2023. Carbohydrate complexity limits microbial growth and reduces the sensitivity of human gut communities to perturbations. *Nat Ecol Evol* 7, 127–142. <https://doi.org/10.1038/s41559-022-01930-9>
- Park, K.Y., Choi, S.Y., Lee, S.H., Kweon, J.H., Song, J.H., 2016. Comparison of formation of disinfection by-products by chlorination and ozonation of wastewater effluents and their toxicity to *Daphnia magna*. *Environmental Pollution* 215, 314–321. <https://doi.org/10.1016/j.envpol.2016.04.001>
- Qin, W., Hammes, F., 2021. Substrate Pre-loading Influences Initial Colonization of GAC Biofilter Biofilms. *Front Microbiol* 11. <https://doi.org/10.3389/fmicb.2020.596156>
- Rashed, M.N., 2013. Organic Pollutants - Monitoring, Risk and Treatment. IntechOpen. <https://doi.org/10.5772/55953>
- Regnery, J., Wing, A.D., Kautz, J., Drewes, J.E., 2016. Introducing sequential managed aquifer recharge technology (SMART) – From laboratory to full-scale application. *Chemosphere* 154, 8–16. <https://doi.org/https://doi.org/10.1016/j.chemosphere.2016.03.097>
- Renaud, B., Martiny, A.C., 2013. Phylogenetic Distribution of Potential Cellulases in Bacteria. *Appl Environ Microbiol* 79, 1545–1554. <https://doi.org/10.1128/AEM.03305-12>
- Schulten, H.-R., 1996. Three-dimensional, Molecular Structures of Humic Acids and Their Interactions with Water and Dissolved Contaminants. *Int J Environ Anal Chem* 64, 147–162. <https://doi.org/10.1080/03067319608028343>
- Shannon, P., Markiel, A., Ozier, O., Baliga, N.S., Wang, J.T., Ramage, D., Amin, N., Schwikowski, B., Ideker, T., 2003. Cytoscape: A software Environment for integrated models of biomolecular interaction networks. *Genome Res* 13, 2498–2504. <https://doi.org/10.1101/gr.1239303>
- Solisio, C., Lodi, A., Borghi, M. Del, 2001. Treatment of effluent containing micropollutants by means of activated carbon. *Waste Management* 21, 33–40. [https://doi.org/https://doi.org/10.1016/S0956-053X\(00\)00069-6](https://doi.org/https://doi.org/10.1016/S0956-053X(00)00069-6)
- Teeling, H., Fuchs, B.M., Becher, D., Klockow, C., Gardebrecht, A., Bennke, C.M., Kassabgy, M., Huang, S., Mann, A.J., Waldmann, J., Weber, M., Klindworth, A., Otto, A., Lange, J., Bernhardt, J., Reinsch, C., Hecker, M., Peplies, J., Bockelmann, F.D., Callies, U., Gerds, G., Wichels, A., Wiltshire, K.H., Glöckner, F.O., Schweder, T., Amann, R., 2012. Substrate-Controlled Succession of Marine Bacterioplankton Populations Induced by a Phytoplankton Bloom. *Science* (1979) 336, 608–611. <https://doi.org/10.1126/science.1218344>

- Vignola, M., Lenselink, J., Quinn, D., Ijaz, U.Z., Pereira, R., Sloan, W.T., Connelly, S., Moore, G., Gauchotte-Lindsay, C., Smith, C.J., 2023. Differential utilisation of dissolved organic matter compound fractions by different biofilter microbial communities. *AQUA - Water Infrastructure, Ecosystems and Society* 72, 1837–1851. <https://doi.org/10.2166/aqua.2023.036>
- Vignola, M., Werner, D., Hammes, F., King, L.C., Davenport, R.J., 2018a. Flow-cytometric quantification of microbial cells on sand from water biofilters. *Water Res* 143, 66–76. <https://doi.org/10.1016/j.watres.2018.05.053>
- Vignola, M., Werner, D., Wade, M.J., Meynet, P., Davenport, R.J., 2018b. Medium shapes the microbial community of water filters with implications for effluent quality. *Water Res* 129, 499–508. <https://doi.org/10.1016/j.watres.2017.09.042>
- Wang, H., Narihiro, T., Straub, A.P., Pugh, C.R., Tamaki, H., Moor, J.F., Bradley, I.M., Kamagata, Y., Liu, W.T., Nguyen, T.H., 2014. MS2 bacteriophage reduction and microbial communities in biosand filters. *Environ Sci Technol* 48, 6702–6709. <https://doi.org/10.1021/es500494s>
- Wu, X., Wu, L., Liu, Y., Zhang, P., Li, Q., Zhou, J., Hess, N.J., Hazen, T.C., Yang, W., Chakraborty, R., 2018. Microbial interactions with dissolved organic matter drive carbon dynamics and community succession. *Front Microbiol* 9. <https://doi.org/10.3389/fmicb.2018.01234>
- Yanagi, Y., Tamaki, H., Otsuka, H., Fujitake, N., 2002. Comparison of decolorization by microorganisms of humic acids with different ¹³C NMR properties. *Soil Biol Biochem* 34, 729–731. [https://doi.org/https://doi.org/10.1016/S0038-0717\(01\)00196-1](https://doi.org/https://doi.org/10.1016/S0038-0717(01)00196-1)
- Yates, C.A., Johnes, P.J., Owen, A.T., Brailsford, F.L., Glanville, H.C., Evans, C.D., Marshall, M.R., Jones, D.L., Lloyd, C.E.M., Jickells, T., Evershed, R.P., 2019. Variation in dissolved organic matter (DOM) stoichiometry in U.K. freshwaters: Assessing the influence of land cover and soil C:N ratio on DOM composition. *Limnol Oceanogr* 64, 2328–2340. <https://doi.org/10.1002/lno.11186>

Graphical Abstract



Declaration of interests

The authors declare that they have no known competing financial interests or personal relationships that could have appeared to influence the work reported in this paper.

The authors declare the following financial interests/personal relationships which may be considered as potential competing interests:

Journal Pre-proof